

One dimensionality and spectroscopy in carbon nanotubes*

C. KRAMBERGER[†]

University of Vienna, Strudlhofgasse 4, A-1090 Vienna, Austria

Unlike regular three-dimensional solids two of a nanotube dimensions are confined and quantized. Bulk samples consist of irregular networks of merging and splitting bundles of parallel tubes. On a local scale, nanotubes are at the same time one-dimensional crystals and two-dimensional quantum rings. They have attracted extensive studies on individual aspects in their electronic and optical properties [1]. The current contribution aims at bridging the fundamental physical concepts behind carbon nanotubes to their unique spectroscopic signatures in optical absorption, luminescence, Raman and electron energy loss spectroscopy. The aim is not to compete with the local depth of a focused review, but to briefly convey the physical concept and related spectroscopic signatures of one-dimensionality. Indirect signatures are the manifold appearances of van Hove singularities in their optical transitions. Direct probes of one-dimensionality unveil the confined momentum space, which manifests in the distinction of localized and propagating excitations.

Keywords: carbon nanotube; spectroscopy; one-dimensionality

© Wrocław University of Technology.

1. Electronic structure of carbon nanotubes

Carbon nanotubes exist as multi walled and single walled cylinders made of graphene sheets. In the following we will focus on the archetypical case of single walled carbon nanotubes (SWNTs). In essence every SWNT is an infinitely long stripe of the honeycomb graphene sheet that happens to be rolled up and meet with itself after going around the circumference once. SWNTs are therefore fully described by the lattice vector along the circumference. By these periodic boundary conditions the two-dimensional k-space of graphene is reduced to a set of parallel cuts. This concept of zone folding may be applied to derive any one dimensional quasi-particle (e.g. electrons and phonons) dispersion of nanotubes from the two dimensional dispersion in graphene [2]. Regarding electrons, graphene is a half metal where the valence and the conduction band touch only at two inequivalent points.

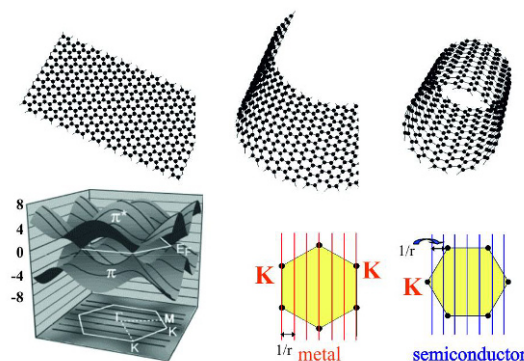


Fig. 1. A rolled up stripe of graphene implies periodicity along the circumference (top row). The 2D hexagonal Brillouin zone is sliced into parallel lines that either hit a K point in a metallic SWNT, or miss it in a semiconducting SWNT (bottom row).

In the vicinity of these K -points the linear two-dimensional bandstructure is the famous *Dirac-cone*.

If the parallel cutting lines of a specific nanotube hit these points or miss them the SWNT is either a metal or a semiconductor. The scheme is illustrated in Fig. 1. In one-dimension the density of states (DOS) diverges in van Hove singularities (VHS) at any flat slope. The continuous DOS of

*This paper was presented at the Conference Functional and Nanostructured Materials, FNMA 12, 23 – 27 September 2012, Aegina Island, Greece

[†]E-mail: Christian.Kramberger-Kaplan@univie.ac.at

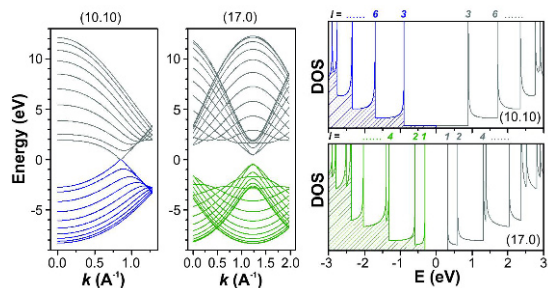


Fig. 2. Left panel: Examples for the electronic bandstructure of a metallic (10,10) armchair SWNT and a semiconducting (17,0) zig-zag SWNT. Right panel: Electronic DOS with the characteristic VHS of the (10,10) and the (17,0) SWNT, respectively.

electrons and phonons is dominated by a discrete set of VHS. In this way a quasi-discrete excitation spectrum emerges within the framework of one-dimensional solids. Smaller SWNT diameters imply larger allowed steps in the circumferential wavevector and hence, further apart cutting lines and an increased spacing of the VHS. The conical slices as well as the DOS of archetypical metallic and semiconducting SWNTs are shown in Fig. 2.

2. Signatures of van Hove singularities

VHS are a consequence of one-dimensionality and have been confirmed and evaluated in great detail by various spectroscopic techniques such as electron energy loss spectroscopy (EELS), Optical absorption spectroscopy (OAS), photoemission, and photoluminescence [3–6]. While the selected spectroscopic methods summarized here confirm VHS, they do not directly probe one-dimensionality. VHS are merely observed as discrete energy levels in the DOS.

Optical spectroscopies use visible or near visible electromagnetic waves to interact with the specimen. In OAS the absorption processes occurring due to optical transitions between VHS in the valence and conduction band are a hallmark of SWNT [4]. The observed peaks in Fig. 3 are macroscopic averages over a semitransparent film of SWNT. If a bulk sample provides a blend of

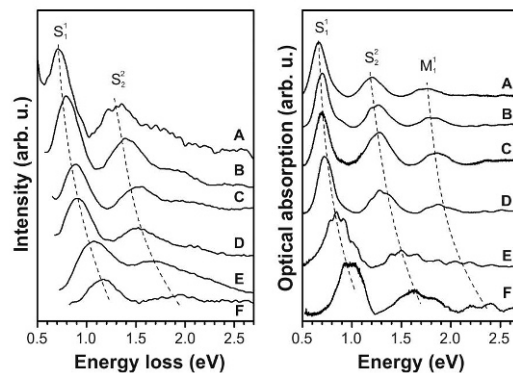


Fig. 3. The peaks in the left panel (EELS) and the right panel (OAS) shift with the mean diameter of the SWNT material. A, B, C, D, E and F label different samples with mean diameters of 1.46, 1.37, 1.34, 1.30, 1.09 and 0.91 nm, respectively.

semiconducting and metallic nanotubes with different diameters, these are reflected in transition energies, relative intensities and width of the cumulative peaks [7]. Fig. 3 also shows a complementary way to excite interband transition, in EELS [3]. In EELS, interband excitations are not created upon absorption of an incoming photon but by scattering a relativistic electron inelastically. Scattering events with relativistic electrons are due to long range Coulomb interaction and can hence also probe the density dependent dielectric background. The surrounding charges lead to a stiffening of the electronic excitations, which manifests in an up-shift as compared to absorption spectroscopy.

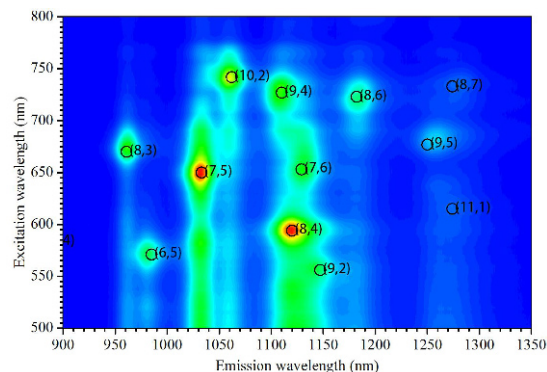


Fig. 4. Photoluminescence map of a SWNT. The marks label pairs of transitions between second and first VHS in a semiconducting SWNT.

Photoluminescence (PL) is another optical probe of the interband transition between VHS in carbon nanotubes [6]. PL requires an isolated semi-conducting SWNT. In the process the incoming light is absorbed into a higher VHS, the hot electron then cools down and re-emits a photon from the first VHS. If the tubes are metallic or adjoining one, the excited electron recombines with the hole without emitting light. An example of a PL map is shown in Fig. 4.

Raman spectroscopy on SWNT bears similarities to either OAS and EELS [8]. Here, visible light is used as a probe like in OAS and inelastic scattering takes place as in EELS. However, scattering occurs not on interband excitations but on phonons. Raman active phonons in SWNT comprise the radial breathing mode (RBM), the D-line and the G-line as well as the respective overtones. A typical Raman spectrum is shown in Fig. 5. The frequency of the RBM is of special interest since it scales as the inverse of SWNT diameter. The ratio of the D-line to the G-line is also an established (but arbitrary) measure of defect concentration. The D-line would not be Raman active in an ideal geometry, but it may be activated by lattice defects.

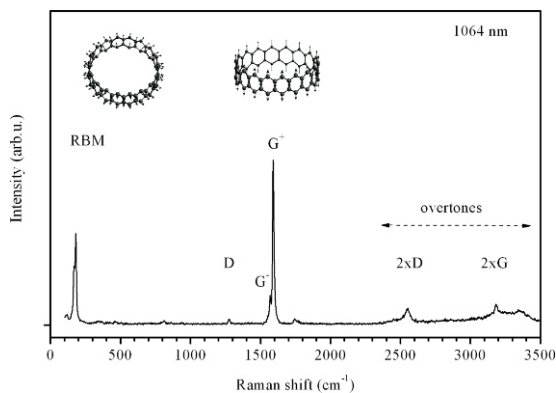


Fig. 5. Raman spectrum of SWNT. The insets show the displacement patterns of the RBM and the G mode, respectively.

Raman scattering does not only reveal phonons but also the optical transitions that match the used laser light. The Raman spectrum is always dominated by the response of those SWNTs whose optical transitions are in resonance with the impinging laser (or the scattered light). Therefore differ-

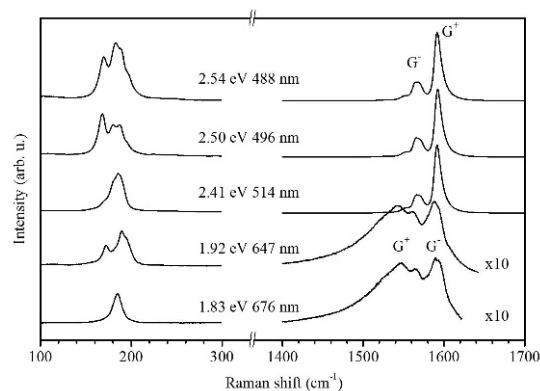


Fig. 6. Multi frequency resonance Raman spectra of a bulk SWNT sample. At each excitation wavelength only the resonant SWNTs show up in the spectra.

ent SWNTs come into resonance and the Raman spectra change when different laserlines are used in Fig. 6.

3. Signatures of one dimensionality

While VHS are a hallmark of SWNTs and can be well explained within the framework of one-dimensional solids. A direct proof of spectroscopic one-dimensionality requires to go beyond optical transitions between VHS. The momentum of light is approximately three orders of magnitude smaller than a solid's Brillouin zone. This minute momentum is simply insufficient to probe the actual dimensionality. In an angle resolved EELS (AR-EELS) experiment the incoming electron has an initial momentum typically hundred times larger than the Brillouin zone [9]. In such an experiment one can look beyond discrete optical transitions into the full dispersion relation of the electronic excitations [10].

AR-EELS on SWNT sees VHS (see Fig. 3) as well as plasmons (density waves) due to the resonances of π and σ electrons, respectively. These plasmons are present in graphite and nanotubes likewise. The different densities in graphite, bulk bundled SWNTs and freestanding isolated SWNTs result in different dielectric backgrounds and signs

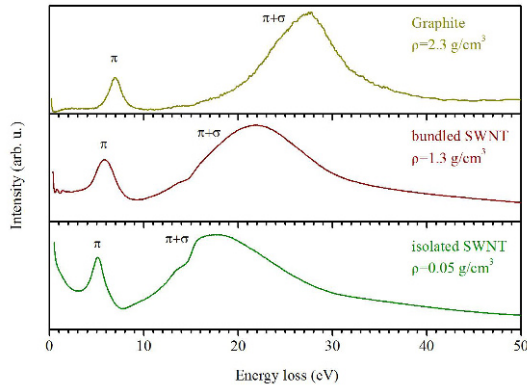


Fig. 7. The archetypical loss-function of sp^2 carbon comprises the collective π and σ plasmons. Their positions scale down with the lower density in graphite, consolidated bundled SWNT, and freestanding isolated SWNT.

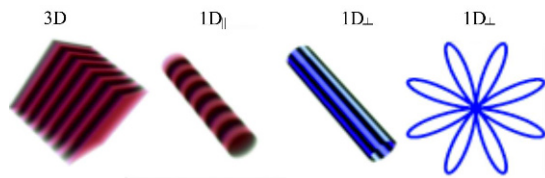


Fig. 8. Charge density patterns of plasmons. From left to right: plane waves in the bulk, plane wave on a wire, circumferential localized plasmon mode and polar plot of the charge density in the latter.

responsible for the shift revealed in Fig. 7. Regarding one-dimensionality, collective density waves on a nanotube are in analogy to the zone-folding scheme split into running waves along the axis and standing waves that are quantized around the circumference.

The density patterns for regular bulk plasmons as well as for the plasmons on a wire are illustrated in Fig. 8. The former will show a dispersion and the latter will be invariant with momentum transfer q in an inelastic scattering experiment.

The loss-function of isolated freestanding nanotubes with increasing momentum transfers q is displayed in Fig. 9. While there is only one plasmon observed at small q , higher q reveal a twofold nature. One plasmon stays in place and a second one disperses to higher energies. These two intrinsically different behaviors are the fingerprint of plas-

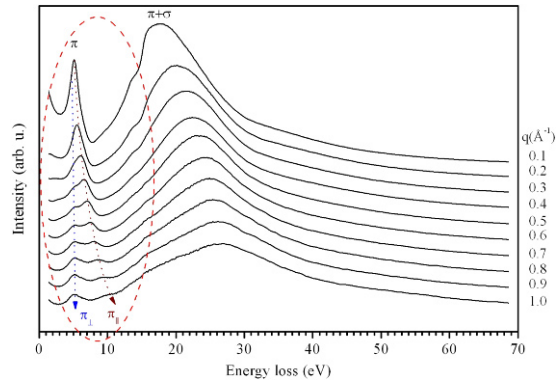


Fig. 9. The loss-function of isolated SWNT at various momentum transfers. The arrows mark the localized π_{\perp} and dispersive π_{\parallel} plasmons.

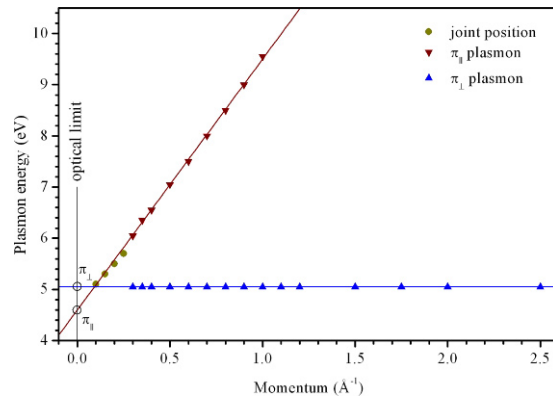


Fig. 10. The linear dispersion of the on-axis π_{\parallel} and the constant dispersion of the localized π_{\perp} plasmon cross one another at a finite momentum. At low q the two π plasmons are no longer resolved.

mons on a quantum wire mentioned afore. The evaluated dispersion relation is shown in Fig. 10. The slope of the dispersive π_{\parallel} plasmon is found to be constant with a value of $v = 4.9 \text{ eV}\text{\AA}$ and an optical limit ($q \rightarrow 0$) of 4.6 eV. The optical limits match the peak positions found in polarized OAS on a freestanding SWNT [11]. The full width half maximum of the individual plasmons is of the order of $2\pi \cdot \tau = 1.5 \text{ eV}$. If the entire π plasmon was modeled with one single damped oscillator, the typical lifetime and speed of propagation would yield a mean free path of $v \cdot \tau > 20 \text{ \AA}$. This value is the minimal coherence length if only a single oscil-

lator and lifetime extension would be considered. The actual shape contributions from the joint density of states will effectively lead to a longer coherence length.

The twofold π plasmon dispersion relation proves that in isolated nanotubes charge density waves may indeed only propagate along the axis, which is an immediate consequence of one-dimensionality.

Acknowledgements

The author acknowledges support through an APART fellowship (11456) of the Austrian Academy of Science.

References

- [1] JORIO A., DRESSELHAUS S., DRESSELHAUS G. (Eds.), *Carbon Nanotubes Advanced Topics in the Synthesis, Structure, Properties and Applications*, Topics in applied Physics 111, Springer Verlag, Berlin Heidelberg, 2008.
- [2] HAMADA N., SAWADA S., OSHIYAMA A., *Phys. Rev. Lett.*, 68 (1992), 1579.
- [3] PICHLER T., KNUPFER M., GOLDEN M.S., FINK J., RINZLER A., SMALLEY R.E., *Phys. Rev. Lett.*, 80 (1998), 4729.
- [4] KATAURA H., KUMAZAWA Y., MANIWA Y., UMEZU I., SUZUKI S., OTHSUKA Y., ACHIBA Y., *Synth. Met.*, 103 (1999), 2555.
- [5] ISHII H. et al., *Nature*, 426 (2003), 540.
- [6] BACHILO S.M., STRANO M.S., KITTEL C., HAUGE R.H., SMALLEY R.E., WEISMAN R.B., *Science*, 298 (2002), 2361.
- [7] LIU X., PICHLER T., KNUPFER M., GOLDEN M.S., FINK J., KATAURA H., ACHIBA Y., *Phys. Rev. B*, 66 (2002), 045411.
- [8] HIURA H., EBBESEN T.W., TANIGAKI K., TAKAHASHI H., *Chem. Phys. Lett.*, 202 (1993) 509.
- [9] FINK J., *Adv. Elec. and Elec. Phys.*, 75 (1989), 121.
- [10] KRAMBERGER C. et al., *Phys. Rev. Lett.*, 100, (2008), 196803.
- [11] MURAKAMI Y., EINARSSON E., EDAMURA T., MARUYAMA S., *Phys. Rev. Lett.*, 94 (2005), 087402.

Received 2012-12-07
Accepted 2013-04-04